Electronic Supplementary Material (ESI) for Journal of Materials Chemistry A.

Supporting Information

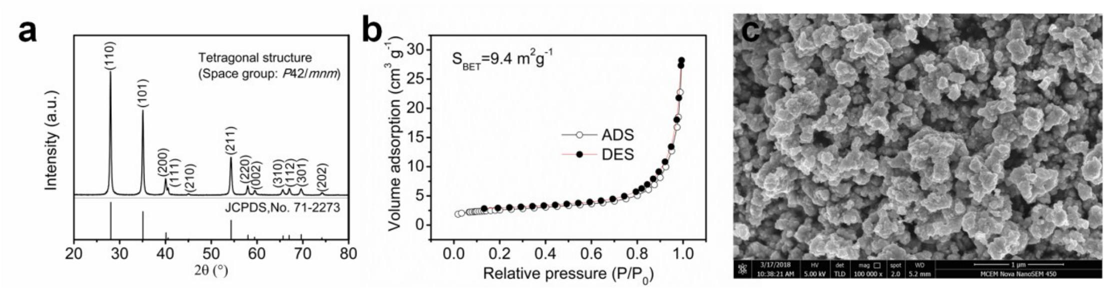

Fig. S1. (a) XRD patterns of commercial RuO_2 powder (Sigma-Aldrich). (b) N_2 adsorption-desorption isotherm of RuO_2. (c) SEM image of RuO_2.

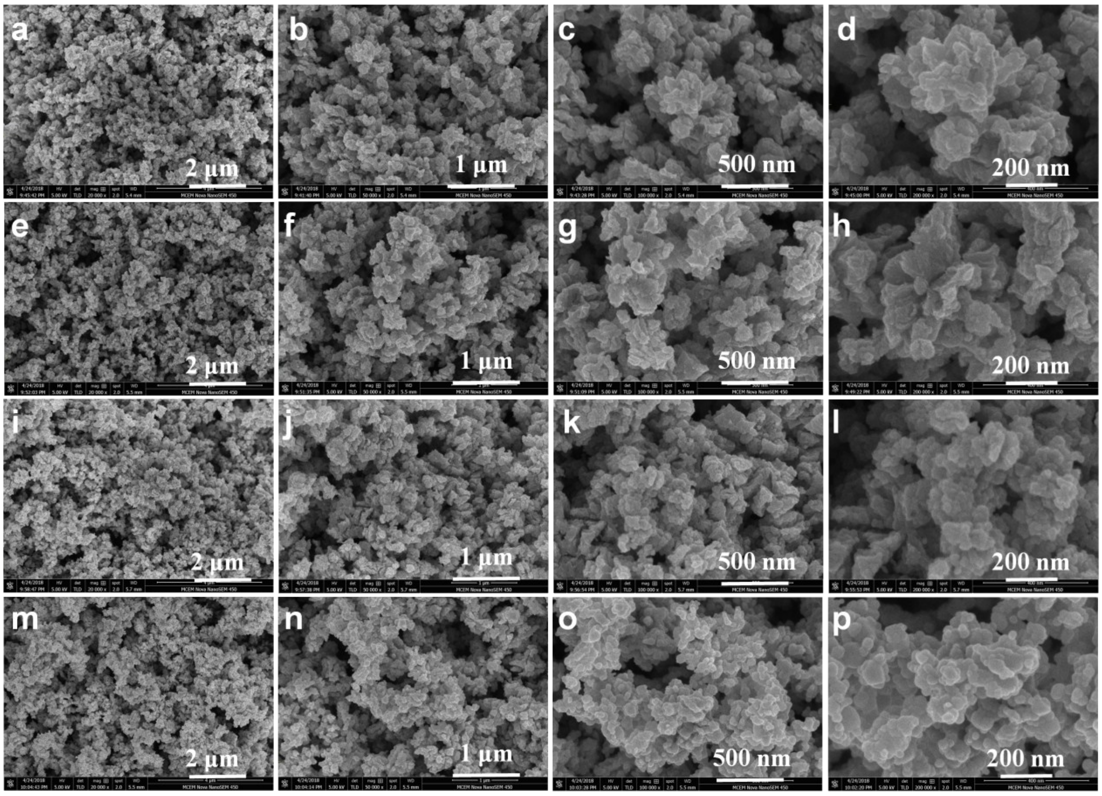

Fig. S2. SEM images with different magnifications of (a-d) RuS_2-400, (e-h) RuS_2-500, (i-l) RuS_2-600 and (m-p) RuS_2-700.

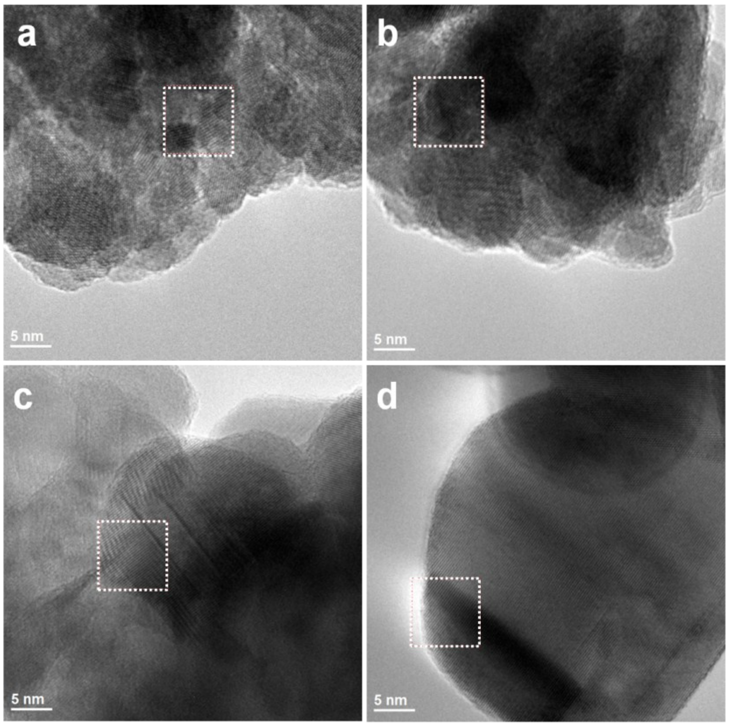

Fig. S3. HRTEM images of (a) RuS_2-400, (b) RuS_2-500, (c) RuS_2-600 and (d) RuS_2-700.

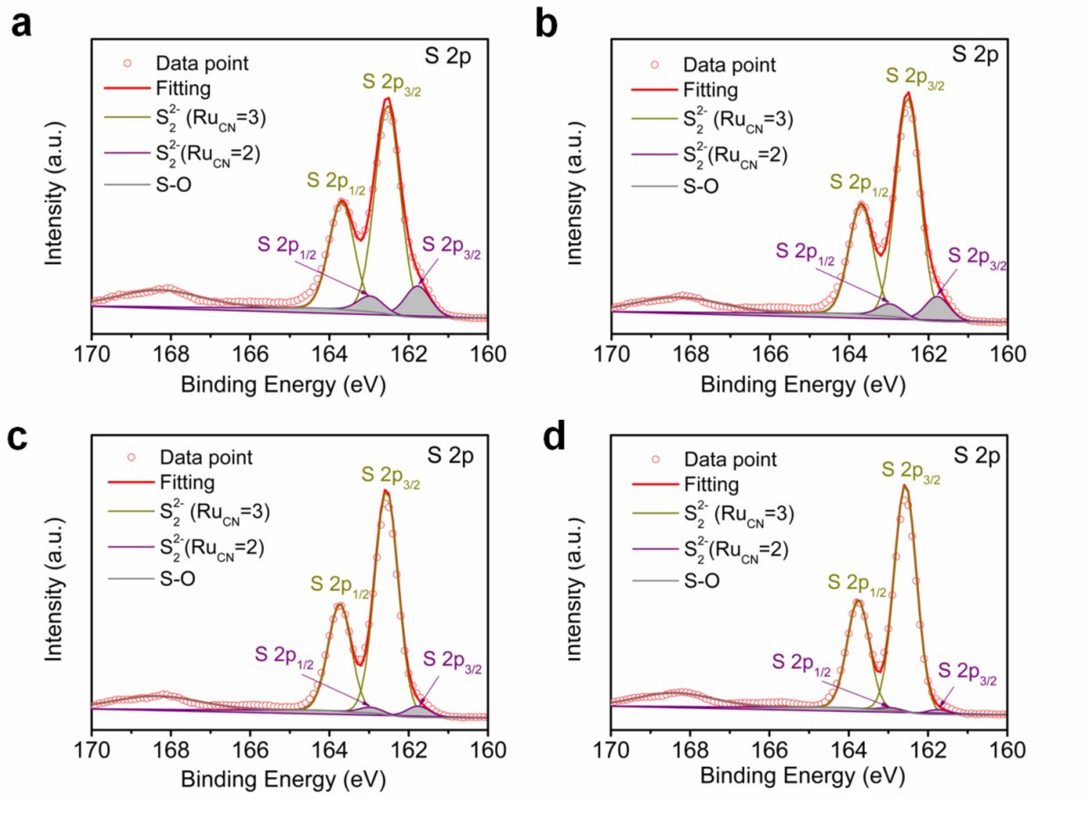

Fig. S4. Deconvoluted XPS S 2p spectra of (a) RuS_2-400, and (b) RuS_2-500, (c) RuS_2-600 and (d) RuS_2-700.

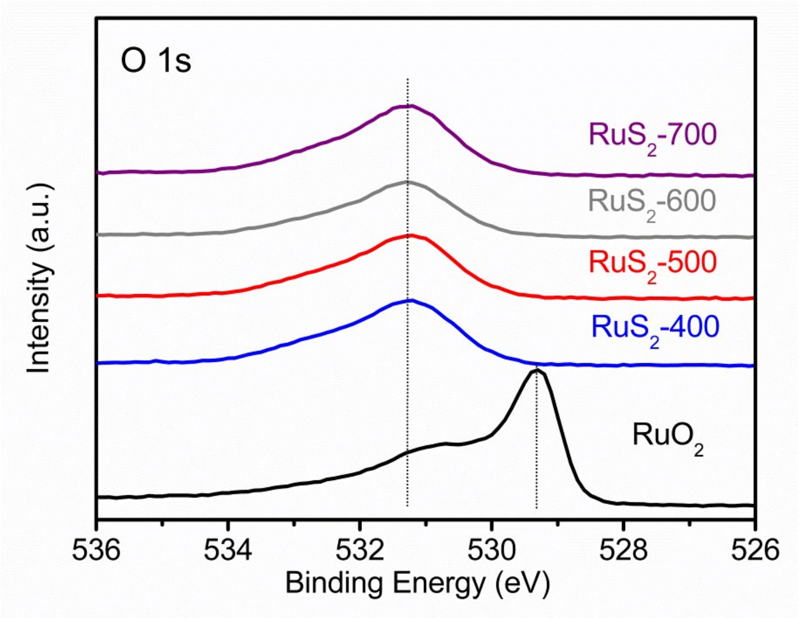

Fig. S5. XPS spectra of O1s for RuS_2-T and RuO_2.

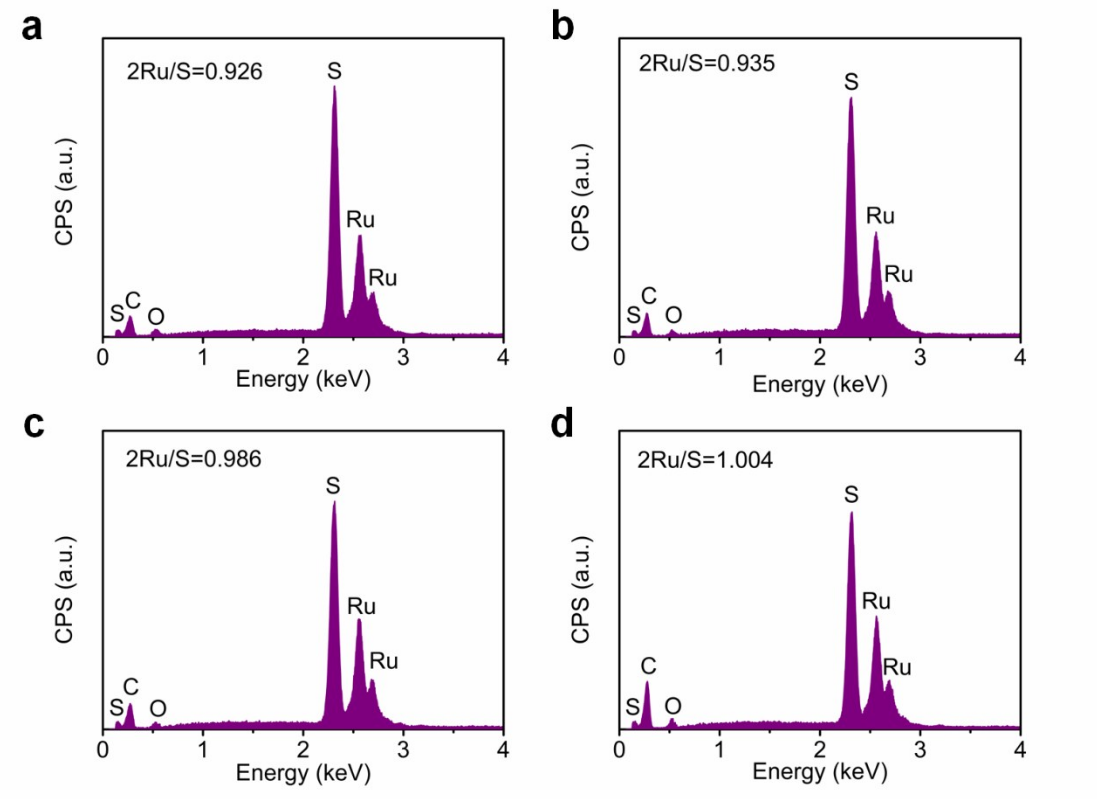

Fig. S6. EDX spectra of (a) RuS_2-400, and (b) RuS_2-500, (c) RuS_2-600 and (d) RuS_2-700.

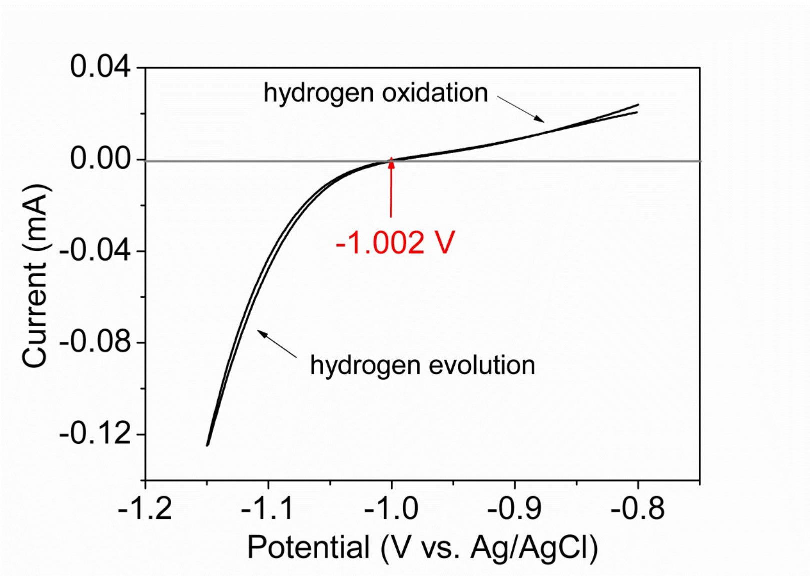

Fig. S7. Potential calibration of the Ag/AgCl reference electrode in 1 M KOH solution. The calibration was performed in a high purity hydrogen-saturated electrolyte with a platinum rotating disk electrode (PINE, 4 mm diameter, 0.126 cm^2) as the working electrode. Cyclic voltammetry (CV) was run at a scan rate of 1 mV s^{-1}, and the average of the two potentials at which the current crossed zero was taken to be the thermodynamic potential for the hydrogen electrode reaction. In 1 M KOH, $E_{RHE} = E_{Ag/AgCl} + 1.002$ V.

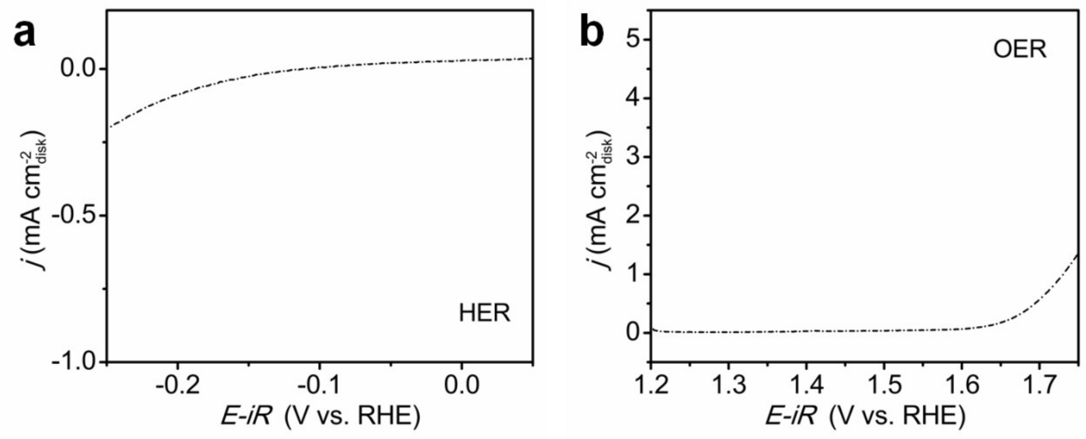

Fig. S8. (a) HER and (b) OER polarization curve of conductive carbon in 1 M KOH.

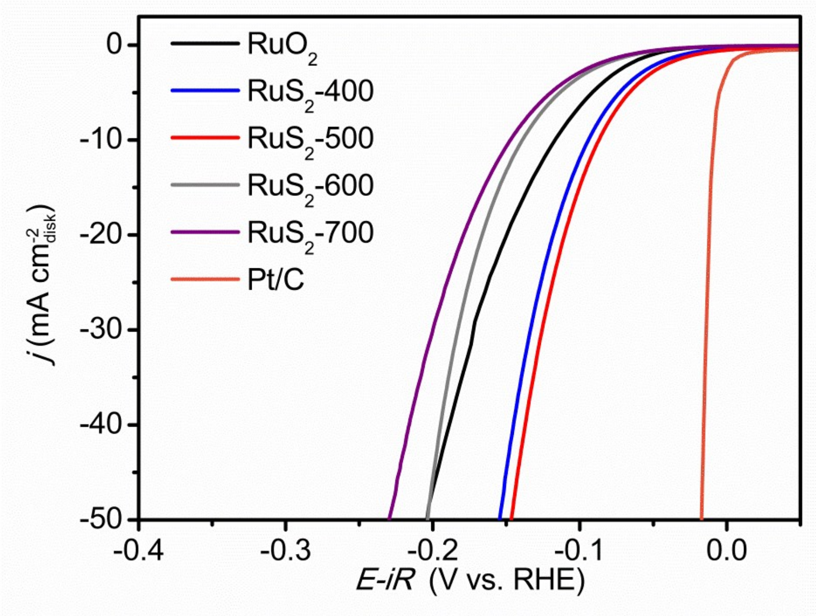

Fig. S9. HER polarization curves of RuS_2-T, RuO_2 and Pt/C catalysts in Ar-saturated 0.5 M H_2SO_4 solution. Scan rate, 5 mV s^{-1}.

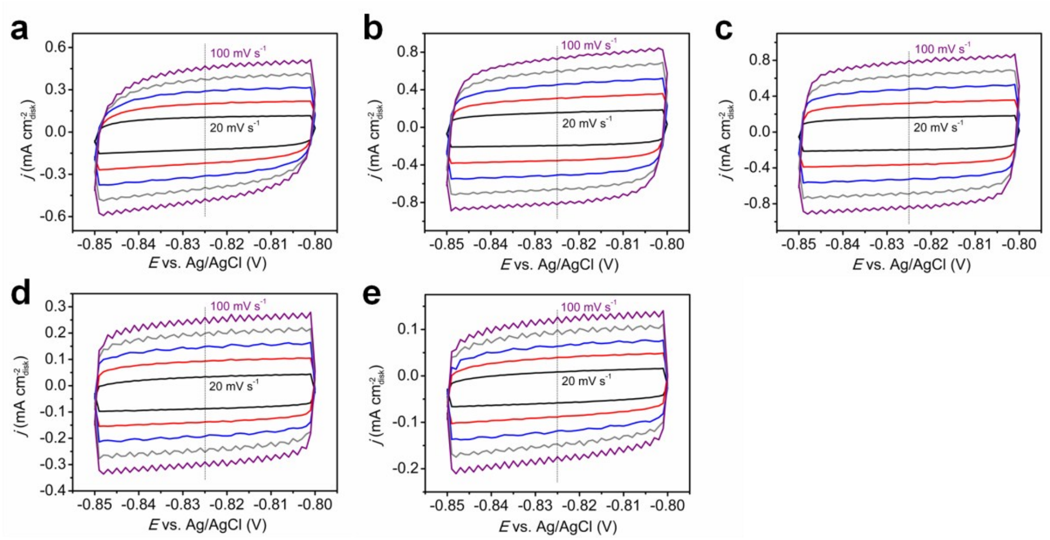

Fig. S10. CV measurements in a non-faradic current region (-0.85--0.8 V vs. Ag/AgCl) at scan rates of 20, 40, 60, 80 and 100 mV s^{-1} of (a) RuO_2, (b) RuS_2-400, (c) RuS_2-500, (d) RuS_2-600 and (e) RuS_2-700 catalysts in 1 M KOH solution.

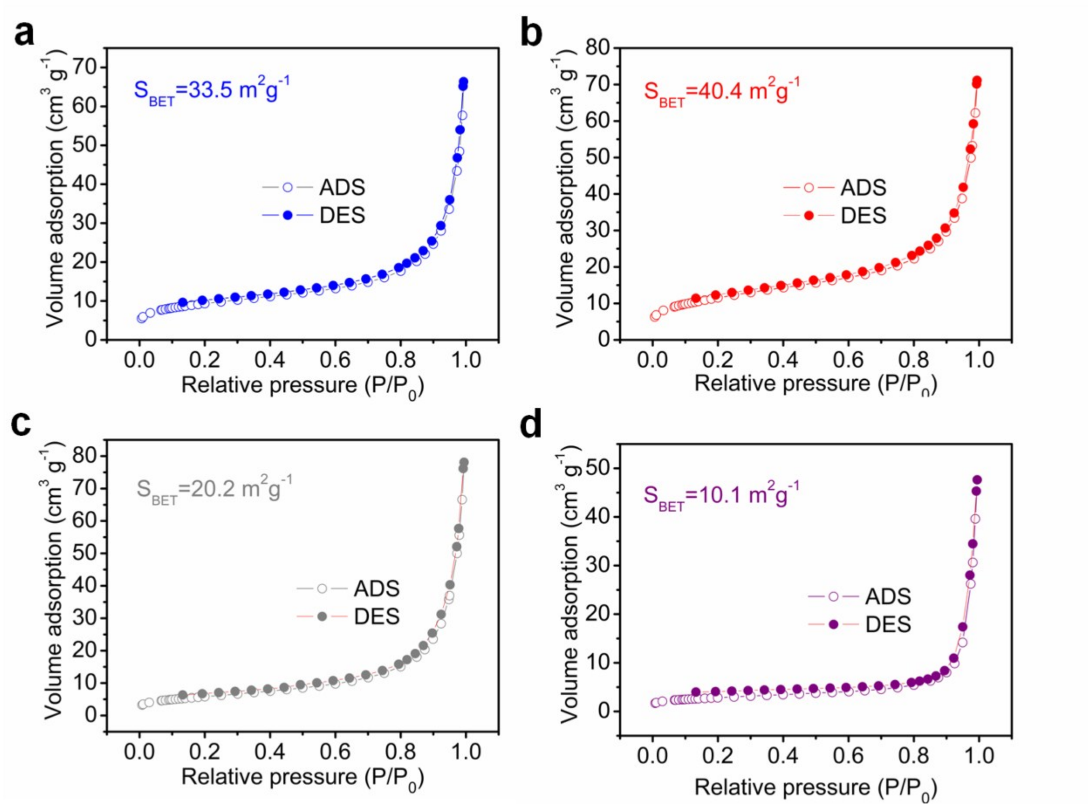

Fig. S11. N_2 adsorption-desorption isotherm of (a) RuS_2-400, (b) RuS_2-500, (c) RuS_2-600 and (d) RuS_2-700.

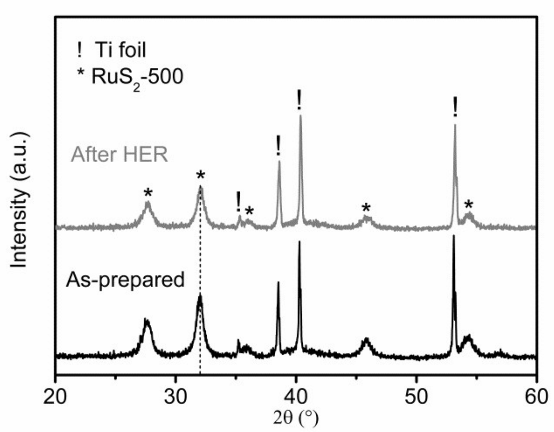

Fig. S12. XRD patterns of RuS_2-500 loaded on the Ti foil substrate before and after HER for 50 cycles. The XRD patterns show that there is no apparent variation in the peak pattern and position between as-prepared and post-HER RuS_2-500, revealing the unchanged bulk crystal structure of RuS_2-500 during HER.

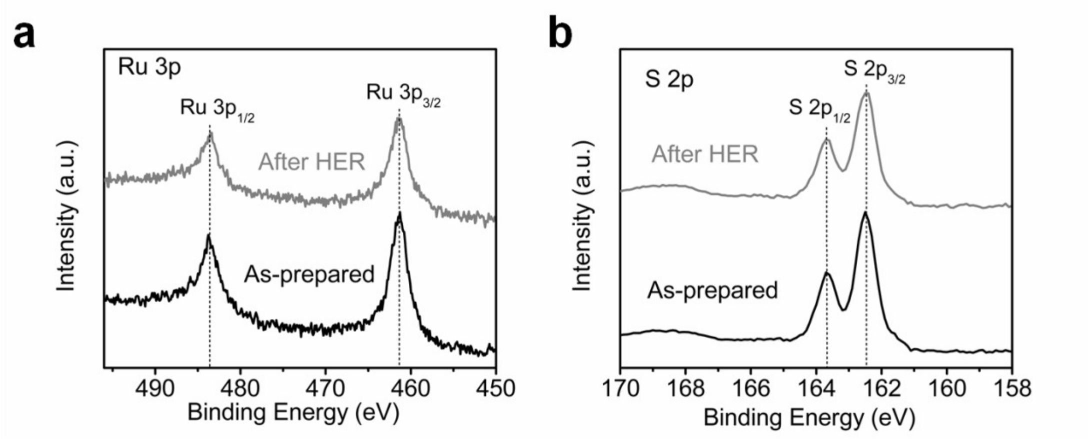

Fig. S13. XPS spectra of (a) Ru 3p and (b) S 2p for RuS_2-500 before and after HER for 50 cycles. XPS spectra of Ru 3p and S 2p show almost no change after HER for 50 cycles.

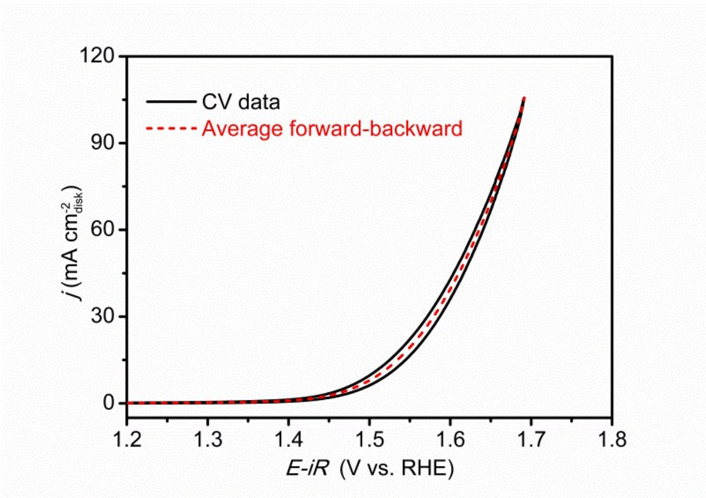

Fig. S14. Capacitive correction of the as-measured CV curve (10 mV s^{-1}) of example catalyst (i.e., RuS_2-500).

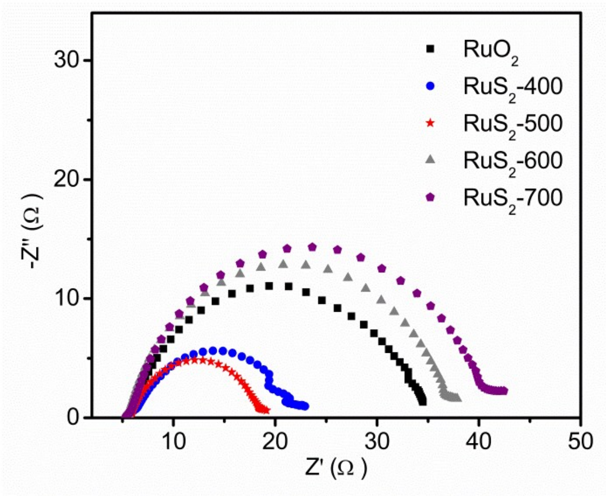

Fig. S15. Nyquist plots of RuO_2, RuS_2-400, RuS_2-500, RuS_2-600 and RuS_2-700 catalysts recorded at 0.6 V vs. Ag/AgCl (no iR-corrected) under the influence of an AC voltage of 10 mV.

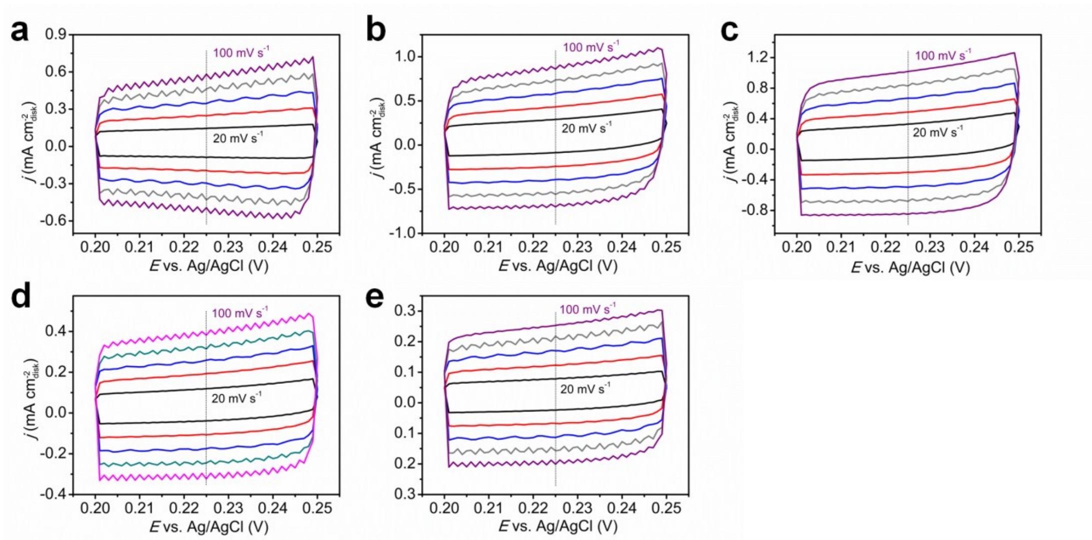

Fig. S16. CV measurements in a non-faradic current region (0.2-0.25 V vs. Ag/AgCl) at scan rates of 20, 40, 60, 80 and 100 mV s^{-1} of (a) RuO_2, (b) RuS_2-400, (c) RuS_2-500, (d) RuS_2-600 and (e) RuS_2-700 catalysts in 1 M KOH solution.

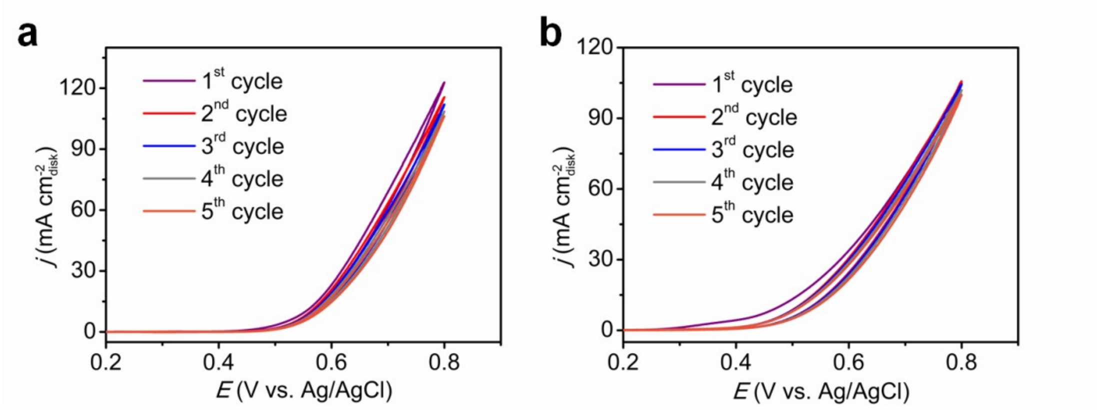

Fig. S17. Cyclic voltammograms of (a) RuO_2 and (b) RuS_2-500 for 5 cycles within OER potential window.

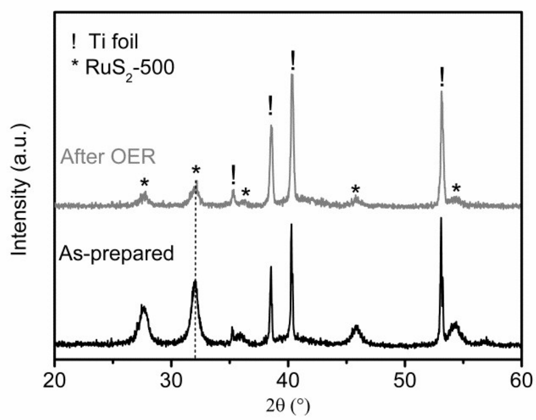

Fig. S18. XRD patterns of RuS_2-500 loaded on the Ti foil substrate before and after OER for 50 cycles.

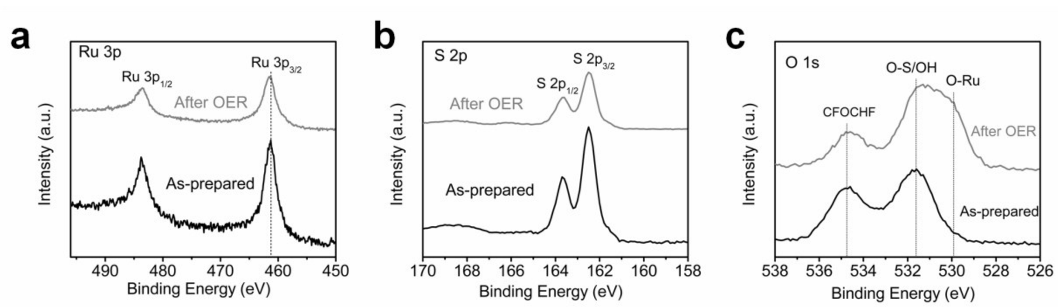

Fig. S19. XPS spectra of (a) Ru 3p, (b) S 2p and (c) O 1s for RuS_2-500 before and after HER for 50 cycles. The peak of Ru $3p_{3/2}$ slightly shifts to higher energy for post-OER samples, indicating partial oxidation on the surface. In O 1s, the peak at ~534.8 eV is originating from the CFOCHF of Nafion solution[1,2] which was included in the electrode preparation. The peaks at ~529-530 eV are associated with the lattice oxygen in metal oxides[3-5].

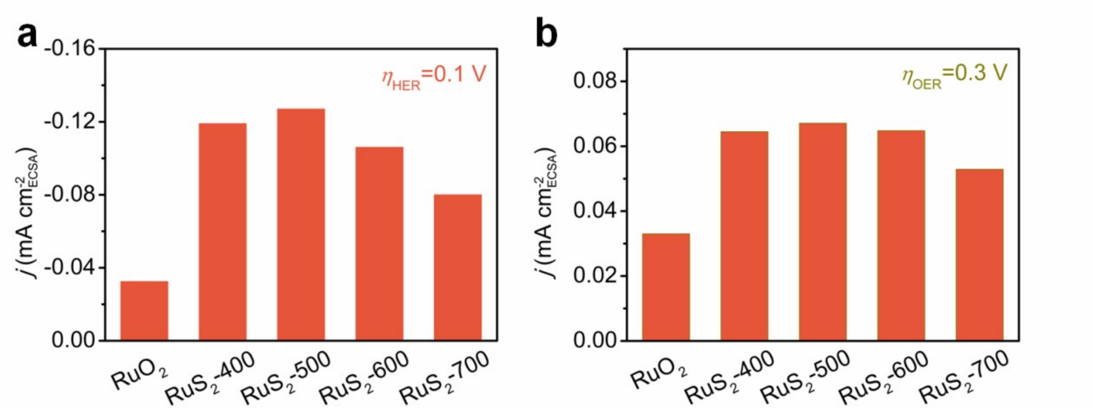

Fig. S20. Intrinsic activity of RuO_2 and RuS_2-T for (a) HER and (b) OER.

Table S1. Position annihilation lifetime parameters of RuS_2-T samples.

Samples	τ1 (ns)	τ2 (ns)	τ3 (ns)	I1 (%)	I2 (%)	I3 (%)
RuS_2-400	0.18±0.03	0.350±0.007	1.61±0.14	17±5	82±5	1.2±0.2
RuS_2-500	0.20±0.02	0.358±0.007	1.61±0.17	18±5	81±5	1.1±0.2
RuS_2-600	0.20±0.02	0.355±0.009	1.55±0.18	23±6	76±6	1.1±0.2
RuS_2-700	0.20±0.02	0.349±0.01	1.84±0.24	27±7	72±7	1.0±0.2

Table S2. S 2p XPS peak deconvolution results.

Samples	S_2^{2-} (Ru_{CN}=3)	S_2^{2-} (Ru_{CN}=2)	S-O
RuS_2-400	75.4%	11.2%	13.4%
RuS_2-500	78.5%	9.0%	12.5%
RuS_2-600	83.1%	4.3%	12.6%
RuS_2-700	85.9%	1.9%	12.2%

Table S3. Comparison of HER activity for RuS_2-500 and well-known Ru-based/pyrite-based catalysts in 1 M KOH.

Catalysts	Substrate	Mass loading ($mg\cdot cm^{-2}$)	η @ -10 mA cm^{-2} (mV)	Tafel slope (mV dec^{-1})	References
RuS_2-500	**Glass carbon**	**0.278**	**79**	**50**	**This work**
Ru-based catalysts					
$Ru@C_2N$	N.A.[a]	0.285	17	38	*Nat. Nanotech.* **2017**, 12, 441
$Ru@TiO_2$[b]	Glass carbon	0.255	110	95	*J. Am. Chem. Soc.* **2018**, 140, 5719
$RuP_2@NPC$	Glass carbon	1	52	69	*Angew. Chem. Int. Ed.* **2017**, *56*, 11559
RuP	Ni foam	0.21	168	123	*Adv. Energy Mater.* **2018**, 8, 1801478
Pyrite-based catalysts					
Mesoporous FeS_2[b]	Ni foam	0.53	96	78	*J. Am. Chem. Soc.* **2017**, 139, 13604
NiS_2/CoS_2-O NW	CFP	0.218	174	45	*Adv. Mater.* **2017**, 29, 1704681
2D NiS_2	Ni foam	1.6	122	86	*Nano Energy* **2017**, 41, 148
V-doped NiS_2	Glass carbon	0.272	110	90	*ACS Nano* **2017**, 11, 11574
$Ni_{0.33}Co_{0.67}S_2$ NW	Ti foil	0.3	88	118	*Adv. Energy Mater.* **2015**, *5*, 1402031
$Pt@CoS_2$	Carbon cloth	0.5	24	82	*Adv. Energy Mater.* **2018**, 8, 1800935
$Co_{0.97}V_{0.03}SP$	Glass carbon	0.28	105	65	*Adv. Energy Mater.* **2018**, 8,1702139
$Co(S_xSe_{1-x})_2$	Ni foam	1	122	86	*Adv. Funct. Mater.* **2017**, 27, 1701008
o-$CoSe_2$|P	Glass carbon	1.02	104	69	*Nat. Commun.* **2018**, *9*, 2533
c-$CoSe_2$	Carbon cloth	0.5	200	85	*Adv. Mater.* **2016**, 28, 7527
$Ni_{0.89}Co_{0.11}Se_2$ MNS	Ni foam	2.62	85	52	*Adv. Mater.* **2017**, 29, 1606521
Tubular $CoSe_2$ NS	Ni foam	N.A	79	84	*Angew. Chem. Int. Ed.* **2018**, 130, 7775
$Ni_{0.33}Co_{0.67}Se_2$	CFP	N.A	106	60	*Adv. Energy Mater.*, **2017**, 7, 1602089

Note: NW, Nanowire; MNS, Mesoporous nanosheet; NS, Nanosheet; CFP, Carbon fiber paper. [a]: N. A.=Not available. [b]: The electrolyte is 0.1 M KOH.

Table S4. Comparison of OER activity for RuS_2-500 and well-known Ru-based/pyrite-based catalysts in 1 M KOH.

Catalysts	Substrate	Mass loading ($mg{\cdot}cm^{-2}$)	η @ 10 mA cm^{-2} (mV)	Tafel slope (mV dec^{-1})	References
RuS_2-500	**Glass carbon**	**0.278**	**282**	**105**	**This work**
Ru-based catalysts					
Ru-Ni SN	Glass carbon	0.1	310	75	*Nano Energy* **2018**, 47, 1
Ru-RuP_x-Co_xP	Glass carbon	N.A.[a]	291	85	*Nano Energy* **2018**, 47, 270
$Pb_2Ru_2O_{6.5}$[b]	Glass carbon	0.637	~410	114	*Energy Environ. Sci.,* **2017**, 10, 129
Pyrite-based catalysts					
Bulk CoS_2	Glass carbon	0.8	480	160	*Angew. Chem. Int. Ed.* **2017**, 56, 4858
$Ni_{6/7}Fe_{1/7}S_2$	Glass carbon	0.2	350	69	*Adv. Mater.* **2018**, 30, 1800757
$FeNiS_2$ NS	Glass carbon	0.1	410	135	*Nano Energy* **2018**, 43, 300
Pt-CoS_2	Carbon cloth	0.5	300	58	*Adv. Energy Mater.* **2018**, 8, 1800935
$NiSe_2$	Glass carbon	0.255	344	91	*Nano Energy.* **2018**, 47, 275
Ag-$CoSe_2$	Glass carbon	0.2	320	56	*Angew. Chem., Int. Ed.* **2017**, 56, 328
$Au_{25}/CoSe_2$[b]	Glass carbon	0.2	410	80	*J. Am. Chem. Soc.,* **2017**, 130, 1077
$Mn_3O_4/CoSe_2$[b]	Glass carbon	0.2	450	49	*J. Am. Chem. Soc.,* **2012**, 134, 2930
SUC $CoSe_2$	Glass carbon	0.17	~350	64	*Angew. Chem. Int. Ed.* **2015**, 54, 12004

Note: SN, Sandwiched nanoplate; NS, Nanosheet; SUC, Single-unit-cell.

[a]: N. A.=Not available. [b]: The electrolyte is 0.1 M KOH.

Table S5. Summary of overall-water-splitting performance in 1 M KOH of various state-of-the-art bifunctional electrocatalysts.

Bifunctional catalysts	Substrate	Mass loading ($mg \cdot cm^{-2}$)	$E_{J=10}$ (V)	Durability (h)	References
RuS_2-500	**CP**	**1.5**	**1.527**	**20**	**This work**
Ru or Pyrite-based catalysts					
RuP	Ni foam	0.21	1.61	12	*Adv. Energy Mater.* **2018**, 8, 1801478
Ru-Ni SN	CFP	3	1.58	40	*Nano Energy* **2018**, 47, 1
c-$CoSe_2$	Carbon cloth	0.5	1.63	~2.8	*Adv. Mater.* **2016**, 28, 7527
NiS_2/CoS_2–O	CFP	N.A.	~1.77	21	*Adv. Mater.* **2017**, 29, 1704681
V-doped NiS_2	Ni foam	1	1.56	20	*ACS Nano* **2017**, 11, 1157
Pt-CoS_2	Carbon cloth	0.5	1.55	20	*Adv. Energy Mater.* **2018**, 8, 1800935
$Co(S_xSe_{1-x})_2$	Ni foam	1	1.63	20	*Adv. Funct. Mater.* **2017**, 27, 1701008
Other state-of-the-art bifunctional catalysts					
NiFe LDH[c]	Ni foam	N. A.	1.70	10	*Science* **2014**, 345, 1593
FeS NS	Iron foam	N.A.	1.65	50	*Chem* **2018**, 4, 1139
2-cycle $NiFeO_x$ NP	CFP	3	1.51	200	*Nat. Commun.* **2015**, 6, 7261
NiFe-MOF	Ni foam	N.A.	1.55	20	*Nat. Commun.* **2017**, 8, 15341
IFONFs-45	Fe foil	N.A.	1.58	8.3	*Nat. Commun.* **2018**, 9, 1809
Ni_3S_2	Ni foam	1.6	~1.76	150	*J. Am. Chem. Soc.* **2015**, 137, 14023
CoO_x/NC	Ni foam	2	1.55	2.5	*J. Am. Chem. Soc.* **2015**, 137, 2688
CoP/NCNHP	Carbon paper	2	1.64	36	*J. Am. Chem. Soc.* **2018**, 140, 2610
CoMnCH	Ni foam	5.6	1.68	13	*J. Am. Chem. Soc.* **2017**, 139, 8320
Holey NiCoP NS	Ni foam	N.A.	1.56	6	*J. Am. Chem. Soc.* **2018**, 140, 5241
MoS_2/Ni_3S_2	Ni foam	9.7	1.56	10	*Angew. Chem. Int. Ed.* **2016**, 55, 6702

Ni_5P_4	Ni foil	~3.5	~1.69	N. A.	*Angew. Chem. Int. Ed.* **2015**, 54, 12361
NiSe NW	Ni foam	2.8	1.63	20	*Angew. Chem. Int. Ed.* **2015**, 54, 9351
Co-P film	Cu foils	1	~1.64	24	*Angew. Chem. Int. Ed.* **2015**, 54, 6251
Hierarchical $NiCo_2O_4$	Ni foam	1	1.65	15	*Angew. Chem. Int. Ed.* **2016**, 55, 6290
$FeSe_2$	Ni foam	3	1.72	24	*Angew. Chem. Int. Ed.* **2017**, 56, 10506
$CoSn_2$	Ni foam	3	1.55	16	*Angew. Chem. Int. Ed.* **2018**, 130, 15457
Porous MoO_2	Ni foam	N. A.	1.53	24	*Adv. Mater.* **2016**, 28, 3785
Fe-CoP	Ti foil	1.03	1.6	40	*Adv. Mater.* **2017**, 29, 1602441
Ni@NC-800	Ni foam	0.8	1.6	50	*Adv. Mater.* **2017**, 29, 1605957
$FePO_4$ NW	Ni foam	0.285	1.54	15	*Adv. Mater.* **2017**, 29, 1704574
Se-$(NiCo)S_x/(OH)_x$ NS	Ni foam	N.A.	1.6	66	*Adv. Mater.* **2018**, 30, 1705538
Ni_3Se_2/Co_9S_8	Exfoliated graphene foil	2.5	1.62	10	Nano Lett. **2017**, 17, 4202
Ni_2P NP	Ni foam	5	1.63	10	*Energy Environ. Sci.* **2015**, 8, 2347
$Co_{0.85}Se$/NiFe-LDH	Exfoliated graphene foil	4	1.67	10	*Energy Environ. Sci.* **2016**, 9, 478
ONPPGC/OCC	Carbon cloth	0.1	1.66	10	*Energy Environ. Sci.* **2016**, 9, 1210
NiFe LDH/Cu NW	Cu foam	2.2	1.54	48	*Energy Environ. Sci.* **2017**, 10, 1820
Ni-Co-P HNB	Ni foam	2	1.62	20	*Energy Environ. Sci.,* **2018**,11, 872
Ni-P($Ni_{11}(HPO_3)_8(OH)_6$	Ni foam	3	1.65	100	*Energy Environ. Sci.,* **2018**, 11, 1287
Co-S@CT	Carbon paper	0.32	1.74	~2 h	*ACS Nano* **2016**, 10, 2342
NiFeSP	Ni foam	4.2	1.58	20	*ACS Nano* **2017**, 11, 10303
CoP NR	Ni foam	6.2	1.62	32	*Adv. Funct. Mater.* **2015**, 25, 7337
NiFe/$NiCo_2O_4$	Ni foam	N. A.	1.67	10	*Adv. Funct. Mater.* **2016**, 26, 3515

Ni-P	CFP	25.8	1.63	100	*Adv. Funct. Mater.* **2016**, 26, 4067
$NiCo_2S_4$ NW	Ni foam	N. A.	1.63	50	*Adv. Funct. Mater.* **2016**, 26, 4661
Co_9S_8@NOSC	Ni foam	5	1.6	10	*Adv. Funct. Mater.* **2017**, 27, 1606585
NC-NiCu-NiCuN	Ni foam	N.A.	1.56	50	*Adv. Funct. Mater.* **2018**, 28, 1803278
Co/NBC-900	Ni foam	2	1.68	6	*Adv. Funct. Mater.* **2018**, 28, 1803278
SNCF-NR	Ni foam	3	1.68	30	*Adv. Energy Mater.* **2017**, 7, 1602122
FeB2 NP	Ni foam	0.08	1.57	24	*Adv. Energy Mater.* **2017**, 7, 1700513
NiCoP films	Scrap copper wires	2	1.59	24	*Adv. Energy Mater.* **2018**, 1802615
$Ni_{1-x}Fe_xPS_3$@ MXene	Ni foam	2	1.65	50	*Adv. Energy Mater.* **2018**, 8, 1801127
Ni_2Fe_1-O	Ni foam	~6	1.64	10	*Adv. Energy Mater.* **2018**, 8, 1701347

Note: SN, Sandwiched nanoplate; NS, Nanosheet; NC, N-doped carbon; NCNHP, N-doped carbon nanotube hollow polyhedron; NW, Nanowire; NP, Nanopaticle; HNB, hollow nanobrick; CT, Carbon tube; NR, Nanorod; NOSC, N-, O-, and S-tridoped carbon;

[c]: The electrolyte is 1 M NaOH.

Supplementary References

[1] Schulze, M.; Lorenz, M.; Wagner, N.; Gülzow, E. XPS analysis of the degradation of Nafion. *Fresen. J. Anal. Chem.* **1999**, *365*, 106-113.

[2] Tazi, B.; Savadogo, O. Parameters of PEM fuel-cells based on new membranes fabricated from Nafion®, silicotungstic acid and thiophene. *Electrochim. Acta* **2000**, *45*, 4329-4339.

[3] Tang, X.; Li, Y.; Huang, X.; Xu, Y.; Zhu, H.; Wang, J.; Shen, W. MnO_x-CeO_2 mixed oxide catalysts for complete oxidation of formaldehyde: effect of preparation method and calcination temperature. *Appl. Catal. B: Environ* **2006**, *62*, 265-273.

[4] Karthe, S.; Szargan, R.; Suoninen, E. Oxidation of pyrite surfaces: A photoelectron spectroscopic study. *Appl. Surf. Sci.* **1993**, *72*, 157-170.

[5] Buckley, A. N.; Woods, R. The surface oxidation of pyrite. *Appl. Surf. Sci.* **1987**, *27*, 437-452.